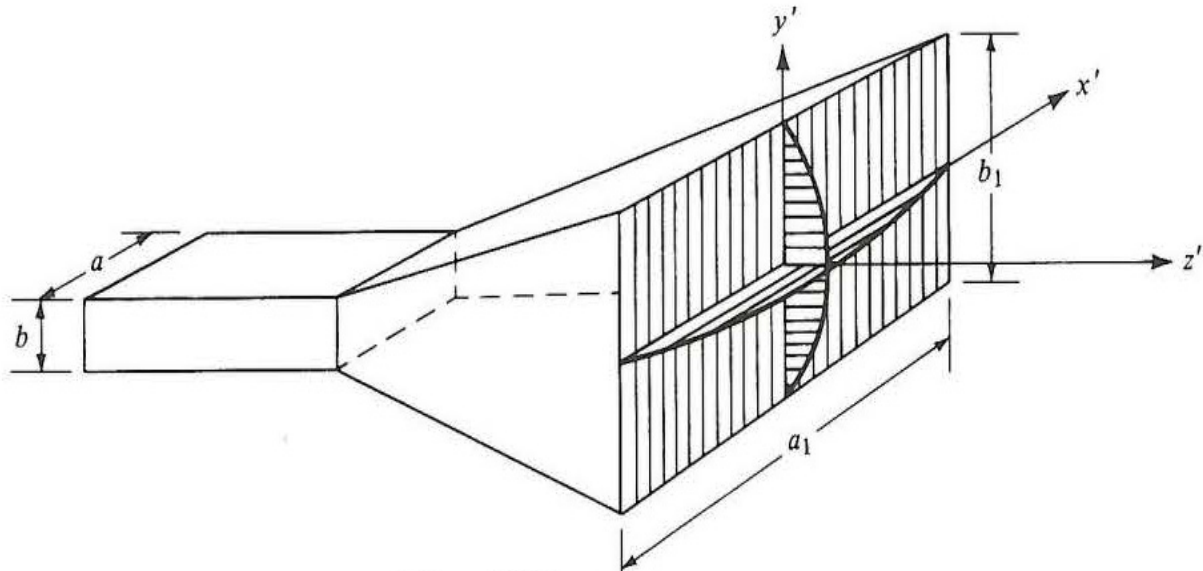


Calculations of Higher Modes in Pyramidal Horn Antennas



By **Hallo Arbely (S2337681)**

Date: July 13, 2015

Supervisors:

Dr. ir. G. de Lange (SRON)

Prof. dr. ir. C.H. van der Wal (RuG)

Dr. T.L.C Jansen (Rug)

Abstract

For this thesis the electric field distribution is calculated on the mouth of the aperture of pyramidal horn antennas. A pyramidal horn is built of flared planes connected to a waveguide. If the field distribution is known, the far field distribution is calculated by the two dimensional Fourier transform, which is represented as the radiation pattern. The final product is a MATLAB code which makes fast plots of radiation pattern for pyramidal horn antennas with specific dimensions. These radiation patterns could be used as comparison material to detected radiation patterns by pyramidal horn antennas.

Acknowledgement

First of all, I thank dr. ir. Gert de Lange who provided insight and expertise that greatly assisted this research.

I thank dr. T.L.C. Jansen for assistance for the computational method and for examining this work and prof. dr.ir. C.H. van der Wal for examining and grading this manuscript.

I would also like to show my gratitude to my colleagues from SRON for sharing their place and wisdom with me during this research.

Thank you all,

Hallo Arbely

Groningen, July 12, 2015

Table of contents

Introduction	4
Antennas	5
Aperture antenna	5
Pyramidal horn antenna	6
Modes	7
Theory	9
Aperture antenna	9
Uniform distribution	9
TE_{10} Mode, plane aperture	10
Pyramidal horn	11
The fundamental mode	11
Higher modes	12
Results	15
Modes appeared in literature	15
Higher modes, pyramidal horn antenna	17
Computational method	18
Conclusions and Discussions	19
References	19
Appendix	20
Derivation of equations [20] and [21]	
Sectoral Horn	
Scripts	

Introduction

In this research project we calculate the way a multi-moded pyramidal horn antenna transmits electromagnetic radiation from free space into a rectangular waveguide. Waveguides are hollow metallic structures with dimensions of order of the tested waves. The waves are from the terahertz region and the corresponding wavelengths is in millimeters. A pyramidal horn is a flared extension of the ends of the waveguide which ends in a bigger aperture. This makes the surface of the detector in the waveguide much bigger. Every antenna has its advantages and disadvantages. Pyramidal horns are simple to design and manufacture. They are designed in rectangular or square shapes. Electromagnetic radiation in the horn is analyzed by taking the solutions of Maxwell's equations as imposed by the metallic sidewalls of the waveguide, which are expressed as modes. Modes are grouped in transverse electric modes, TE , which have no electric fields in the direction of propagation and transverse magnetic, TM , with no magnetic field in the direction of propagation.

The main characteristics of horns are expressed by the so called beam pattern (or radiation pattern) which gives the coupling of electromagnetic field to an antenna as a function of spherical coordinates. Radiation patterns are built of a main lobe and many side lobes. Radiation patterns become narrower when horns are used, because more energy gets in the waveguide. One more benefit of horn antenna is the property of making the translation between free space and waveguide very smooth. Because of this more energy will go through the horn into the waveguide instead of reflection. Because of horns phase error occurs. Phase errors are proportional to the dimension of the aperture of the horn. Greater phase errors cause a wider radiation pattern. This is rectified by making pyramidal horns longer. The dimensions of horn antennas are shown in Figure 3.

To understand this topic some basic cases are developed first. First of all, aperture antennas are discussed. Aperture antennas are pyramidal horn antenna with no horn. After that the pyramidal horns are discussed with constant electric field and field distribution by modes.

The results are mainly based on the analysis as given in Balanis (reference for the fundamental mode of pyramidal horns), and the extension of this analysis as given in the paper of Murphy and Padman as reference for the higher order modes. The basic analysis of the calculation of radiation patterns from aperture antennas can be found in literature, as in optics book by Hecht. The description of diffractions from rectangular and circular apertures are basically a limiting case of the analysis as presented in this thesis. As an introduction to the final results and as a proof of the preciseness of the code, the results obtained are compared to literature values.

From the analysis a final equation is formed which is used to present the asked modes. The used software is MATLAB.

Antennas

1. Aperture antenna

The simplest form of an antenna is the aperture antenna (no horn). Apertures are frequently used as classical examples in optics courses. The definition of the coordinates of the aperture antenna is shown in figure 1, which is also valid for the pyramidal horn antenna discussed later.

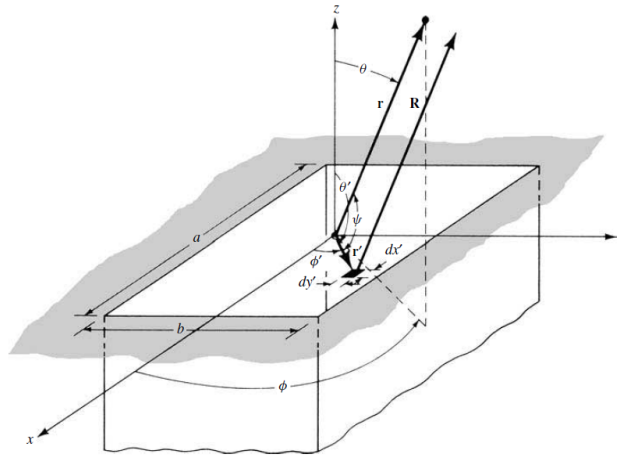


Figure 1 aperture antenna, dimension $a \times b$

The space is defined by the spherical coordinates θ and ϕ and the distance to the source r . θ has the values between $[0, \frac{\pi}{2}]$ and ϕ is $[0, 2\pi]$. The radiation pattern of a square aperture antenna is a sinc function. The derivation is given in literature in optics course book by E. Hecht. The radiation pattern is shown graphically¹ in figure 2.

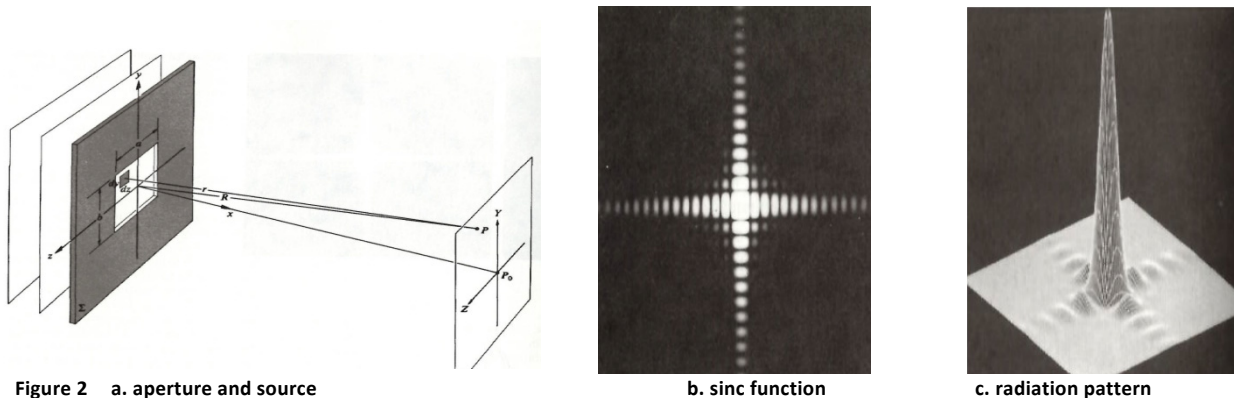


Figure 2 a. aperture and source

b. sinc function

c. radiation pattern

¹ Eugene Hecht, Optics, 4th edition, p. 465,466

2. Pyramidal horn antenna

This chapter starts with a short explanation of the two different types of horn antennas. Pyramidal and sectoral horn antennas. Pyramidal horns are flared in two directions, while sectoral horns are just flared in one direction. The planes of the second direction of the sectoral horn are parallel to each other. If the front side is shown, the aperture of the sectoral horn is as big as the waveguide in one of the directions. The goal of the flaring is receiving more energy because the surface of the aperture is bigger compared to the size of the waveguide. Pyramidal horn antennas are discussed in more detail, while the radiation patterns for the sectoral horn are in the appendix. Sectoral horns are discussed to express the physical properties of pyramidal horn antenna. The difference between sectoral horn and pyramidal horn is schematically given in the next figure.

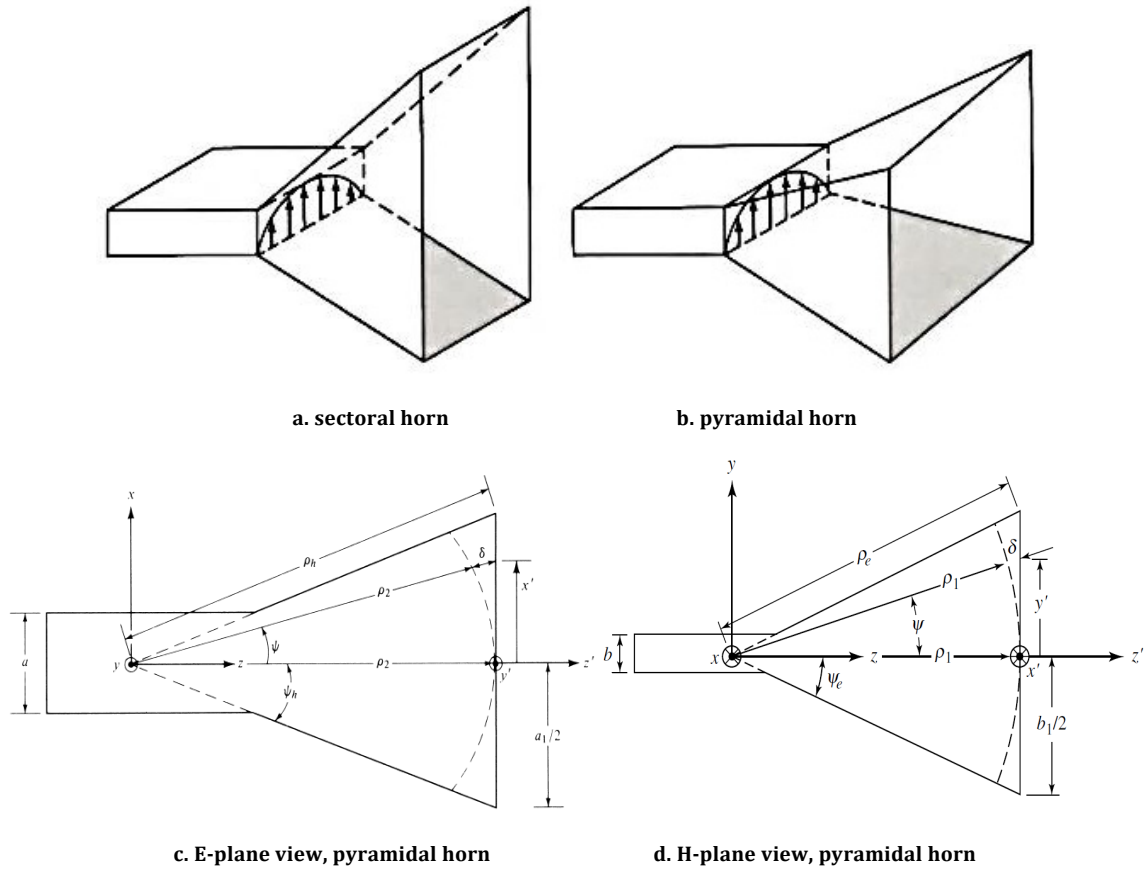


Figure 3.2, Sectoral and pyramidal horn antenna

Because of the flared planes, phase error occurs. This happens as the curved dashed line reach the mouth of the aperture, $y' = 0$, while the curved line of the wave reaches the mouth of the antenna later. The phase error is defined as $\delta\rho = \rho_e - \rho_1$. Which means $\delta\rho$ depends linearly on the size of the aperture. So the phase error is decreased if ρ_1 is longer and the flaring angle is smaller.

² C. Balanis, Antenna theory, 2nd edition, p. 652, 683

Modes

Modes are solutions of wave functions depending on boundary conditions. In this case we look at the solutions of Maxwell's equations on the boundaries of waveguides. The electric field is varying in the horn and is zero at two boundaries. Different modes carry the same amount of energy, but the energy is differently distributed over space. Modes are divided in many groups. Only the relevant ones are discussed here. For this thesis the next two types of modes are taken into account:

- Transverse Electric (TE): this mode has a magnetic field in the direction of propagation, but no electric field in that direction.

$$TE: E^{TE} = A \left[\left(\frac{n}{b} \right) \cos \frac{m\pi x}{a} \sin \frac{n\pi y}{b} \hat{i} + \left(\frac{m}{a} \right) \sin \frac{m\pi x}{a} \cos \frac{n\pi y}{b} \hat{j} \right] \quad [1]$$

- Transverse Magnetic (TM): this mode has an electric field in the direction of propagation, but no magnetic field in that direction.

$$TM: E^{TM} = B \left[\left(\frac{m}{a} \right) \cos \frac{m\pi x}{a} \sin \frac{n\pi y}{b} \hat{i} - \left(\frac{n}{b} \right) \sin \frac{m\pi x}{a} \cos \frac{n\pi y}{b} \hat{j} \right] \quad [2]$$

a and b are the dimensions of the aperture and A and B are constants that are determined by normalizing these functions for values of m and n . The modes are defined in two dimensions, \hat{i} and \hat{j} . It is explained later how the plots are done. Finally, x and y are the boundaries of the aperture.

For each mode a cut off frequency is determined.

$$f_c = \frac{c}{2} \sqrt{\left(\frac{m}{a} \right)^2 + \left(\frac{n}{b} \right)^2} \text{ in (Hz)} \quad , \quad (m, n) = (0, 1, 2, \dots) \text{ and } m = n \neq 0 \text{ for } TE_{mn} \quad [3]$$

$$(m, n) = (1, 2, \dots) \text{ for } TM_{mn}$$

A mode, with specific m and n values, will propagate in a waveguide with dimensions a and b if the cut off frequency of the mode is lower than the frequency of the wave. The dominant mode is defined as the mode with the lowest f_c . For rectangular waveguides this is the TE_{10} , with $m = 1, n = 0$. This mode distributes its energy mostly in the direction of the incoming wave. The remaining energy is distributed everywhere else.

Multi-moded antennas tolerate more than one mode, because their dimension is big enough to do this. Tolerating more modes makes the received signal stronger. The higher the frequency of the received signal the more modes that will propagate through the waveguide upon attenuation. So for the same frequency of the wave, smaller horns can tolerate less modes than greater horns and for two identical horns the same modes are tolerating when different waves are tested. Unless the waves contain enough modes.

The total far-field radiation pattern should contain all the modes, TE & TM , that are propagating in the horn to form the final radiation pattern. Each single mode can be plotted alone to study the contribution. The perfect image is formed when infinite modes are propagating in the horn, which requires very big horns. This case is hard to realize in practice.

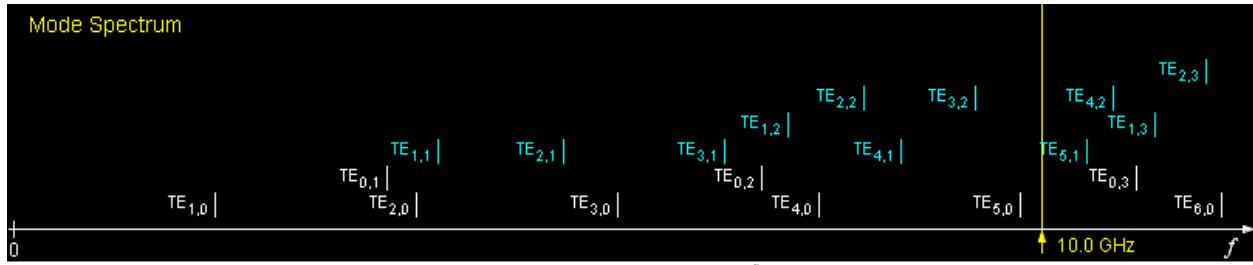


Figure 4, Mode spectrum³ for $\frac{a_1}{b_1} > 1$

The figure above represents the order of appearance of modes in horn antennas. The chosen aperture is rectangular, that is why degenerate modes do not exist. When square apertures are chosen, degenerate modes appear at the same frequency. This is clearly shown by looking at equation [3].

As you can see the fundamental mode is the first mode. All modes to the left of the yellow line, which is the wavelength, are propagating in this horn. The same figure could be obtained for TM_{mn} modes by using the same applet. In addition to the TE_{mn} modes given in blue in figure 4 the same number of TM modes are present. TM_{mn} modes do not exist for indices equal to zero. Equation [2] shows the details. Figure 4 is only shown to make the idea of modes that are propagating in the horn clear.

The regularity in the plots becomes clear if we take a look at upcoming higher modes. The TE_{0n} modes are TE_{m0} modes rotated by $\pi/2$ for $m = n$. The modes with indices not equal to zero, have complex structures. Next, six modes are shown for square apertures.

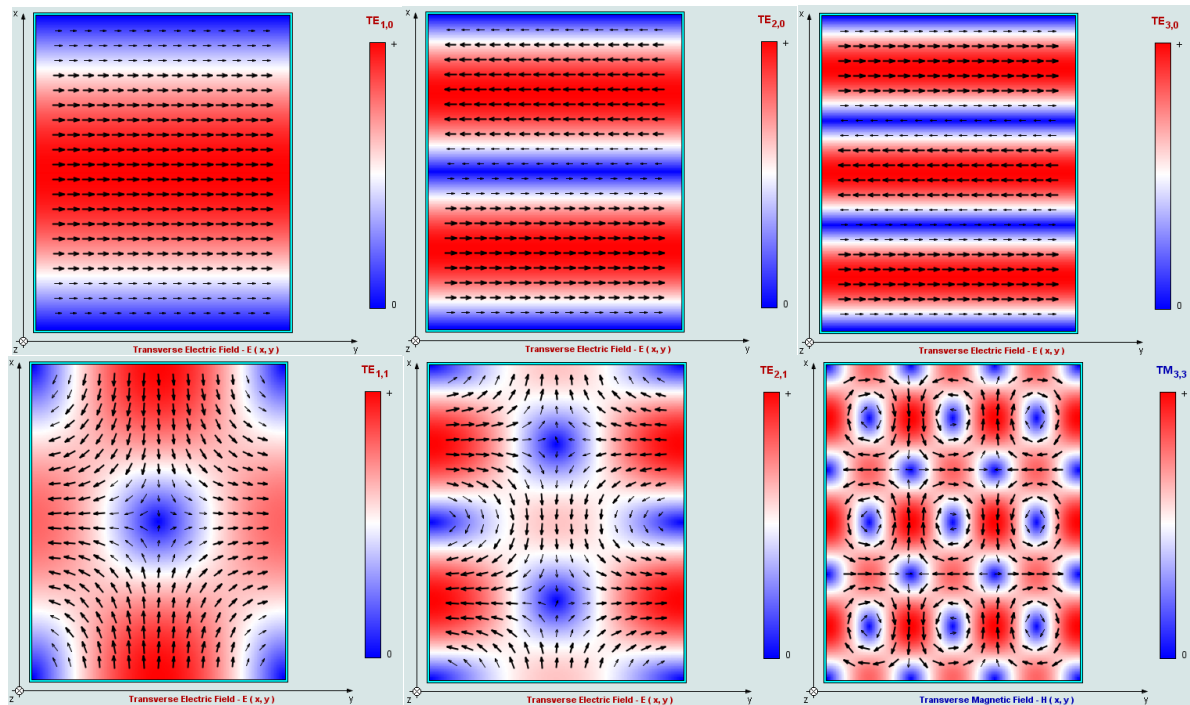


Figure 5, modes a. TE_{10} b. TE_{20} c. TE_{30} d. TE_{11} e. TE_{21} f. TM_{33} (left to right)

³ Applet showing modes, <http://www.amanogawa.com/archive/RectWaveGuide/RectWaveGuide.html>

The electric and magnetic field distributions that are shown in figure 5 are used to determine the far field distribution by applying the two dimensional Fourier transform. In this thesis this is done analytically.

Theory

For this thesis we consider two types of antennas, aperture and pyramidal horn antennas. The difference in design affects the distribution of the field.

1. Aperture antenna: two cases will be considered: uniform and sinusoidal electromagnetic field distributions

- a. Uniform distribution

The field radiated by the aperture is written in terms of its components, which is done in Balanis⁴.

$$E_\theta = i \frac{abkE_0 e^{-ikr}}{2\pi r} \sin \phi \frac{\sin X}{X} \frac{\sin Y}{Y} \quad E_\phi = i \frac{abE_0 e^{-ikr}}{2\pi r} \cos \theta \cos \phi \frac{\sin X}{X} \frac{\sin Y}{Y} \quad E_r = 0 \quad [4]$$

$$\text{Where,} \quad \frac{\sin X}{X} = \text{sinc}(X) \quad \frac{\sin Y}{Y} = \text{sinc}(Y) \quad [5]$$

The angles ϕ and θ cover the whole space and r is the distance from the center of the plane to the source as given in figure 1. a and b are the dimension of the aperture, $k = \frac{2\pi}{\lambda}$ and E_0 is the constant of the field. X and Y are given as following:

$$X = \frac{ka}{2} \sin \theta \cos \phi \quad Y = \frac{kb}{2} \sin \theta \sin \phi \quad [6]$$

The total field distribution, E_{total} , is then:

$$|E_{total}| = \left| \sqrt{E_r^2 + E_\theta^2 + E_\phi^2} \right| = \frac{abkE_0}{2\pi r} \left| \sqrt{(\sin^2 \phi + \cos^2 \theta \cos^2 \phi)} \text{sinc}(X) \text{sinc}(Y) \right| \quad [7]$$

The total electric field distribution is plotted as function of the dimension of the aperture and space coordinates in 3D. The plots give the projection of E_{total} in the x and y axes and E_{total} itself on the z axis.

The projections of E_{total} on the x and y -axes are done by vector analysis from spherical to Cartesian coordinates:

$$x: |E_{total}| \sin \theta \cos \phi \quad \text{and} \quad y: |E_{total}| \sin \theta \sin \phi \quad [8]$$

⁴ C. Balanis, Antenna theory, 2nd edition, p. 588

For a rectangular shaped antenna, $a \neq b$, the following distributions appear

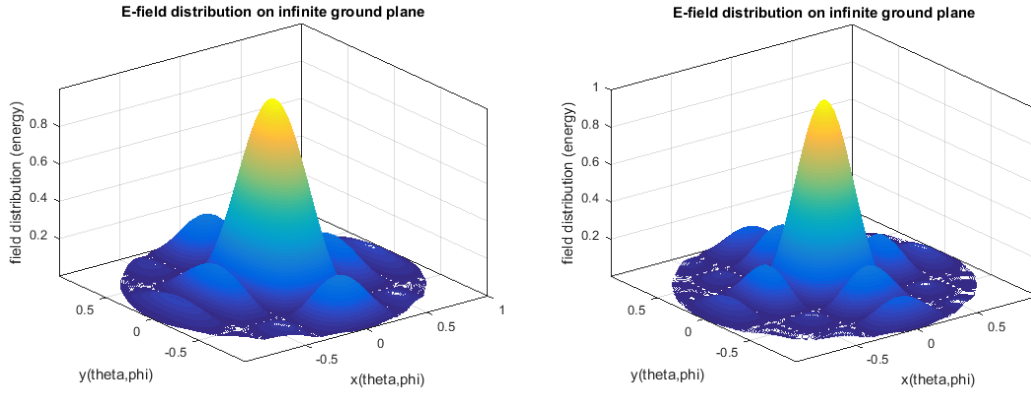


Figure 6,

a. $a = 3\lambda$ and $b = 2\lambda$

b. $a = b = 3\lambda$

The $y - z$ plane, with $x = 0$, is called the E -plane ($\phi = 90^\circ$) and $\phi = 0$ is the H -plane.

The shape of the graphs is not symmetric in different directions. This is because of the different inputs X and Y which are given by equation [6].

These plotted figures are compared with figures given in literature⁵ and the results match.

b. TE_{10} Mode, plane aperture

The last section discussed the uniform distribution on the plane. This section is about electromagnetic distribution at the aperture, which is described by a trigonometric function. This mode covers more than 80% of the energy the waves are carrying in the main direction, the direction where the signal comes in. The formulas of this section are:

$$E_\theta = -i \frac{abE_0\pi e^{-ikr}}{4r} \sin \phi \frac{\cos X}{X^2 - (\frac{\pi}{2})^2} \frac{\sin Y}{Y} \quad E_\phi = -i \frac{abE_0\pi e^{-ikr}}{4r} \cos \theta \cos \phi \frac{\cos X}{X^2 - (\frac{\pi}{2})^2} \frac{\sin Y}{Y} \quad E_r = 0 \quad [9]$$

$$|E_{total}| = \left| \sqrt{E_r^2 + E_\theta^2 + E_\phi^2} \right| = \frac{abE_0\pi}{4r} \left| \sqrt{(\sin^2 \phi + \cos^2 \theta \cos^2 \phi)} \frac{\cos X}{X^2 - (\frac{\pi}{2})^2} \frac{\sin Y}{Y} \right| \quad [10]$$

⁵ C. A. Balanis, Antenna theory, 2nd edition, pages 589 and 590

The figure bellow shows the application of equation [10], the TE_{10} mode.

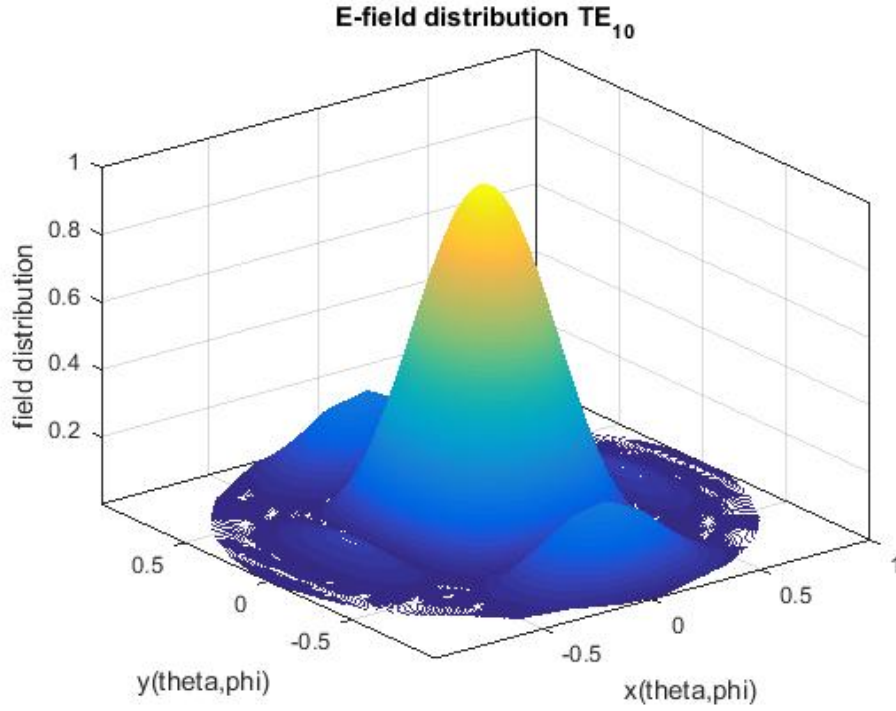


Figure 7, $a = 3\lambda$ and $b = 2\lambda$

2. Pyramidal Horn

The first step toward antennas is adding a horn to the waveguide. With a horn θ , varies between $[0, \pi]$ instead of $[0, \frac{\pi}{2}]$ as in the case of aperture antennas, which means the horn radiates signals in all directions around it.

a. The fundamental mode

As given in Balanis⁶, the equation describing the far field distribution for the fundamental mode, TE_{10} , as function of spherical coordinates and dimensions of the horn, is:

$$|E_{total}| = constant |(1 + \cos\phi)I_1 I_2| \quad [11]$$

Where I_1 and I_2 are

$$I_1 = \frac{1}{2} \sqrt{\left(\frac{\pi \rho_2}{k}\right)} \left(\exp\left(i \frac{k_x'^2 \rho_2}{2k}\right) \{[C(t_2') - C(t_1')] - i(S(t_2') - S(t_1'))\} \right. \\ \left. + \exp\left(i \frac{k_x''^2 \rho_2}{2k}\right) \{[C(t_2'') - C(t_1'')] - i(S(t_2'') - S(t_1''))\} \right) \\ I_2 = \sqrt{\left(\frac{\pi \rho_1}{k}\right)} \left(\exp i \left(\frac{k_y^2 \rho_1}{2k}\right) \{[C(t_2) - C(t_1)] - i(S(t_2) - S(t_1))\} \right) \quad [12]$$

⁶ C. A. Balanis, Antenna theory, 2nd edition, pages 684

And

$$k_y = k \sin \theta \cos \phi \quad k'_x = k \sin \theta \cos \phi + \frac{\pi}{a_1} \quad k''_x = k \sin \theta \cos \phi - \frac{\pi}{a_1} \quad [13]$$

t values depend linearly on $k_{x,y}$ and are used as inputs for the Fresnel integrals which are represented as C and S . The full derivation is given in Balanis.

b. Higher modes

Now it is the task to reconstruct the above equation, equation [11], to contain higher modes. the method used is explained in the article of Murphy⁷. The far field distribution for any mode in the horn is calculated as following

$$E = \text{constant} \left[\iint \text{mode} \exp \left\{ -ik \left(\frac{x^2}{2\rho_2} + \frac{y^2}{2\rho_1} \right) \right\} \exp \{ -ik(\sin \theta \cos \phi x + \sin \theta \sin \phi y) \} dx dy \right] \quad [14]$$

For 'mode' in equation [14] any mode can be chosen from equations [1] and [2]. This derivation is done by taking care of the flaring of the planes of the horn, 1st exponent. As long the angle of the flaring is not too wide, this assumption is valid. For this angle Ψ_e , angles up to 45° are acceptable. The angles, Ψ_e and Ψ_h , are graphically represented in figure 3. The last term in equation [14] is for the two dimensional Fourier transform of the distribution at the mouth of the aperture. In equation [14] each term depends only on x or y , which makes it possible to divide it into two independent parts.

The final equation, written very compact, is of the form:

$$\begin{aligned} P_{mn}^{EH} = \\ \text{const}_1 \left[\iint \cos \frac{m\pi x}{a} \sin \frac{n\pi y}{b} \exp \left\{ -ik \left(\frac{x^2}{2L_x} + \frac{y^2}{2L_y} \right) \right\} \exp \{ -ik(\sin \theta \cos \phi x + \sin \theta \sin \phi y) \} dx dy \right]^2 \end{aligned} \quad [15]$$

$$\begin{aligned} P_{mn}^{HE} = \\ \text{const}_2 \left[\iint \sin \frac{m\pi x}{a} \cos \frac{n\pi y}{b} \exp \left\{ -ik \left(\frac{x^2}{2L_x} + \frac{y^2}{2L_y} \right) \right\} \exp \{ -ik(\sin \theta \cos \phi x + \sin \theta \sin \phi y) \} dx dy \right]^2 \end{aligned} \quad [16]$$

$$P_{total} = \sum P_{mn}^{EH} + \sum P_{mn}^{HE} \quad [17]$$

Equation [14] as given in this thesis gives the electric field distribution of the far field. The same equation is used to give the power distribution, which is the square value of the same equation. In this thesis, equation [14] is used to represent the radiation pattern graphically, this why the equation is given in this form. In the same article, the constant of equation [15] is determined.

⁷ Equation (7) of the same article by A.J. Murphy and R. Padman

The integral is developed by making use of these mathematical rules:

$$\int \cos \frac{n\pi x}{a} \exp \left\{ -ik \left(\frac{x^2}{2L_x} \right) \right\} \exp \{ -ikx \sin \theta \cos \phi \} dx = \frac{1}{2} \sqrt{\left(\frac{\pi \rho_2}{k} \right)} \left(\exp \left(i \frac{k_x'^2 \rho_2}{2k} \right) \{ [C(t'_2) - C(t'_1)] - i(S(t'_2) - S(t'_1)) \} + \exp \left(i \frac{k_x''^2 \rho_2}{2k} \right) \{ [C(t''_2) - C(t''_1)] - i(S(t''_2) - S(t''_1)) \} \right) \quad [18]$$

$$\int \sin \frac{n\pi x}{b} \exp \left\{ -ik \left(\frac{y^2}{2L_y} \right) \right\} \exp \{ -iky \sin \theta \sin \phi \} dy = \frac{1}{2} \sqrt{\left(\frac{\pi \rho_2}{k} \right)} \left(\exp \left(i \frac{k_y'^2 \rho_2}{2k} \right) \{ [C(t'_2) - C(t'_1)] - i(S(t'_2) - S(t'_1)) \} - \exp \left(i \frac{k_y''^2 \rho_2}{2k} \right) \{ [C(t''_2) - C(t''_1)] - i(S(t''_2) - S(t''_1)) \} \right) \quad [19]$$

The fully derivations of the final forms are given in the appendix. Equation [15] becomes

$$E_{mn}^{TE} = const_1 \left[\frac{\pi \sqrt{L_x L_y}}{k} \left\{ \exp \left(i \left(\sin \theta \cos \phi - \frac{m\pi}{a} \right)^2 \frac{\rho_2}{2k} \right) \exp \left(i \left(\sin \theta \sin \phi - \frac{n\pi}{b} \right)^2 \frac{\rho_1}{2k} \right) \exp i \left(\frac{m\pi}{2} + \frac{n\pi}{2} \right) F_1 F_2 \right. \right. \\ \left. \left. + \exp \left(i \left(\sin \theta \cos \phi - \frac{m\pi}{a} \right)^2 \frac{\rho_2}{2k} \right) \exp \left(i \left(\sin \theta \sin \phi + \frac{n\pi}{b} \right)^2 \frac{\rho_1}{2k} \right) \exp i \left(\frac{m\pi}{2} - \frac{n\pi}{2} \right) F_3 F_4 \right. \right. \\ \left. \left. - \exp \left(i \left(\sin \theta \cos \phi + \frac{m\pi}{a} \right)^2 \frac{\rho_2}{2k} \right) \exp \left(i \left(\sin \theta \sin \phi - \frac{n\pi}{b} \right)^2 \frac{\rho_1}{2k} \right) \exp i \left(-\frac{m\pi}{2} + \frac{n\pi}{2} \right) F_5 F_6 \right. \right. \\ \left. \left. - \exp \left(i \left(\sin \theta \cos \phi + \frac{m\pi}{a} \right)^2 \frac{\rho_2}{2k} \right) \exp \left(i \left(\sin \theta \sin \phi + \frac{n\pi}{b} \right)^2 \frac{\rho_1}{2k} \right) \exp -i \left(\frac{m\pi}{2} + \frac{n\pi}{2} \right) F_7 F_8 \right\} \right] \quad [20]$$

And [16] is

$$E_{mn}^{TM} = const_2 \left[\frac{\pi \sqrt{L_x L_y}}{k} \left\{ \exp \left(i \left(\sin \theta \cos \phi - \frac{m\pi}{a} \right)^2 \frac{\rho_2}{2k} \right) \exp \left(i \left(\sin \theta \sin \phi - \frac{n\pi}{b} \right)^2 \frac{\rho_1}{2k} \right) \exp i \left(\frac{m\pi}{2} + \frac{n\pi}{2} \right) F_1 F_2 \right. \right. \\ \left. \left. - \exp \left(i \left(\sin \theta \cos \phi - \frac{m\pi}{a} \right)^2 \frac{\rho_2}{2k} \right) \exp \left(i \left(\sin \theta \sin \phi + \frac{n\pi}{b} \right)^2 \frac{\rho_1}{2k} \right) \exp i \left(\frac{m\pi}{2} - \frac{n\pi}{2} \right) F_3 F_4 \right. \right. \\ \left. \left. + \exp \left(i \left(\sin \theta \cos \phi + \frac{m\pi}{a} \right)^2 \frac{\rho_2}{2k} \right) \exp \left(i \left(\sin \theta \sin \phi - \frac{n\pi}{b} \right)^2 \frac{\rho_1}{2k} \right) \exp i \left(-\frac{m\pi}{2} + \frac{n\pi}{2} \right) F_5 F_6 \right. \right. \\ \left. \left. - \exp \left(i \left(\sin \theta \cos \phi + \frac{m\pi}{a} \right)^2 \frac{\rho_2}{2k} \right) \exp \left(i \left(\sin \theta \sin \phi + \frac{n\pi}{b} \right)^2 \frac{\rho_1}{2k} \right) \exp -i \left(\frac{m\pi}{2} + \frac{n\pi}{2} \right) F_7 F_8 \right\} \right] \quad [21]$$

$$TE: E^{TE} = A \left[\frac{n}{b} E_1 \hat{i} + \frac{m}{a} E_2 \hat{j} \right] \quad TM: E^{TM} = A \left[\frac{m}{a} E_1 \hat{i} - \frac{n}{b} E_2 \hat{j} \right] \quad [22]$$

This is the first part of the final equation.

The sum of these two expressions, E_1 and E_2 , give the field distribution of a mode at the aperture for the far field. F-values are the same in both cases, which are the Fresnel integrals for each ϕ and θ . Any TE_{mn} mode can be formed by adding these two equations together, the same for TM_{mn} modes by subtracting P_{mn}^{HE} from P_{mn}^{EH} . For example, if we take a look at the fundamental mode. If the derivation is correct, equation [14] should be reducible to equation [11]. This is the case since E_{10}^{TM} -modes is equal to zero if $n=0$ and E_{10}^{TE} implies to equation [11]. The derivation is given in the appendix.

The formulas given in the literature contain one more term, $(1 + \cos \theta)$. This is done by taking the components in the ϕ and θ direction of the quantity⁸. The total electric field distribution is then the absolute value of the components. This new expression is extremely helpful. Now higher order modes can be presented graphically.

To plot these functions, the absolute values are needed.

$$E^{TE} \approx \left| \left(\frac{n}{b} E_1 \right)^2 + \left(\frac{m}{a} E_2 \right)^2 \right| \quad E^{TM} \approx \left| \left(\frac{m}{a} E_1 \right)^2 + \left(\frac{n}{b} E_2 \right)^2 \right| \quad [23]$$

Approximation sign is used instead of equal sign because the constants in front of the expression have been omitted.

⁸ Balanis, p. 914

Results

By using the final equation obtained in the last chapter, infinite number of modes are possible to plot. In this chapter only important modes are plotted. These modes are used for discussion and test purposes.

- Modes appeared in literature

First of all, the modes used in Balanis are plotted to justify the code. The next plot shows the radiation pattern for the fundamental mode for these dimensions: $a_1 = 5.5$ and $b_1 = 2.75$ in terms of λ and the axial length of the horn is 6λ in both planes.

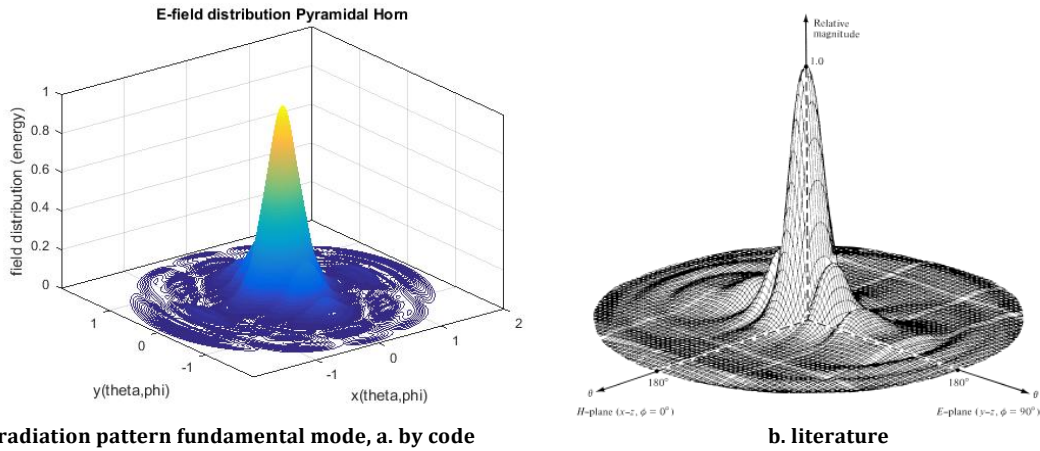


Figure 8, radiation pattern fundamental mode, a. by code

b. literature

The two plots are equivalent to each other by simple observation.

For $a_1 = 12\lambda$, $b_1 = 6\lambda$ and $\rho_1 = \rho_2 = 6\lambda$ the field distribution has two tops, while for dimension used in the last plot, figure 8, only one top occurs.

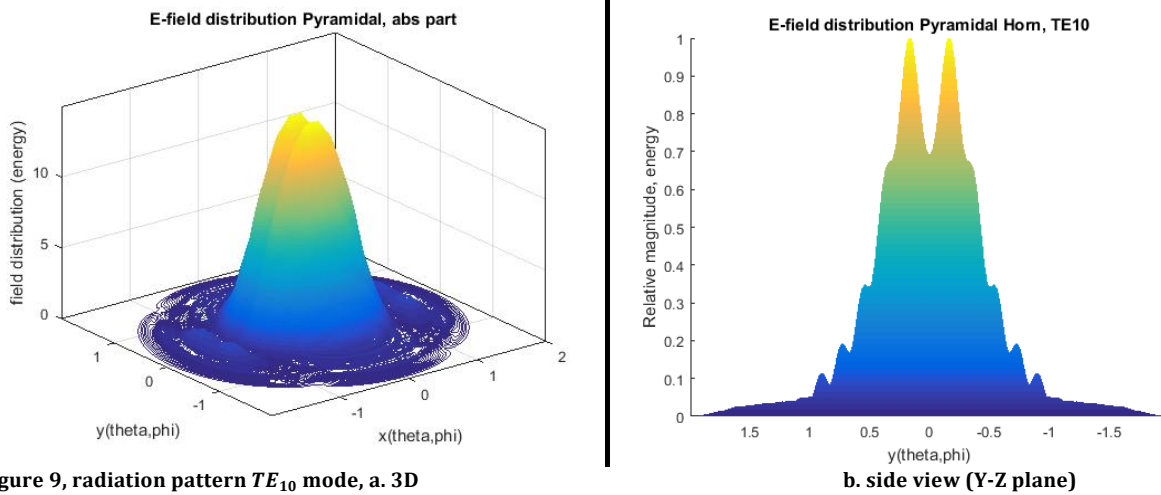


Figure 9, radiation pattern TE_{10} mode, a. 3D

b. side view (Y-Z plane)

The appearance of double top points is due to components which are out of phase with the planes of the horn antenna. The values do not add constructively then.

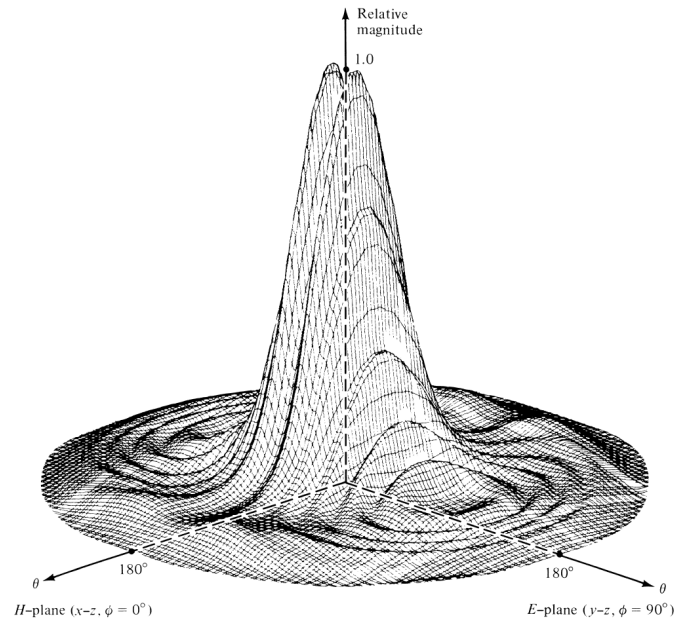


Figure 10, c. literature

With simple observation of figures 10a and 10c, we conclude the equivalence of the plots. Figure 10a is not relativized. The components on the z-axis have values according to the dimension of the antenna. Relativizing the values of the graphs to the maximum value is frequently done in literature.

The intensity plots are given in literature also. This part is of more interest in design theories, which requires side lobe levels of lower than -30 dB. These plots are only given to show the ability of the code to construct these plots, as well.

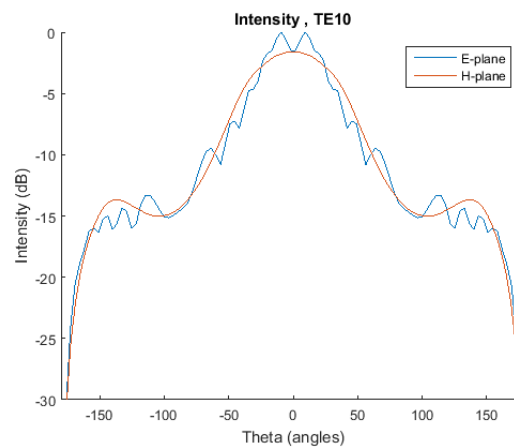


Figure 11, a. Intensity plot

- Higher modes pyramidal horn antenna

It is preferred to show results in surface plots, which make them visually better understood. The difference between surface and contour plots is the projection on the axes. Contour plots represent the physical quantity on the z-axis with the projections of space coordinate on both x and y axes. Surface plots, on the other side, use only projections of the quantity on all axes. The surface plot of the fundamental mode given in figure 8 is shown below.

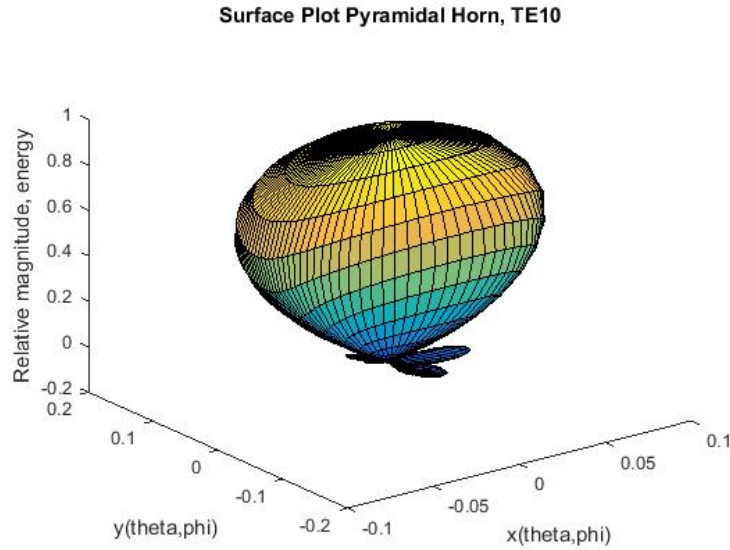
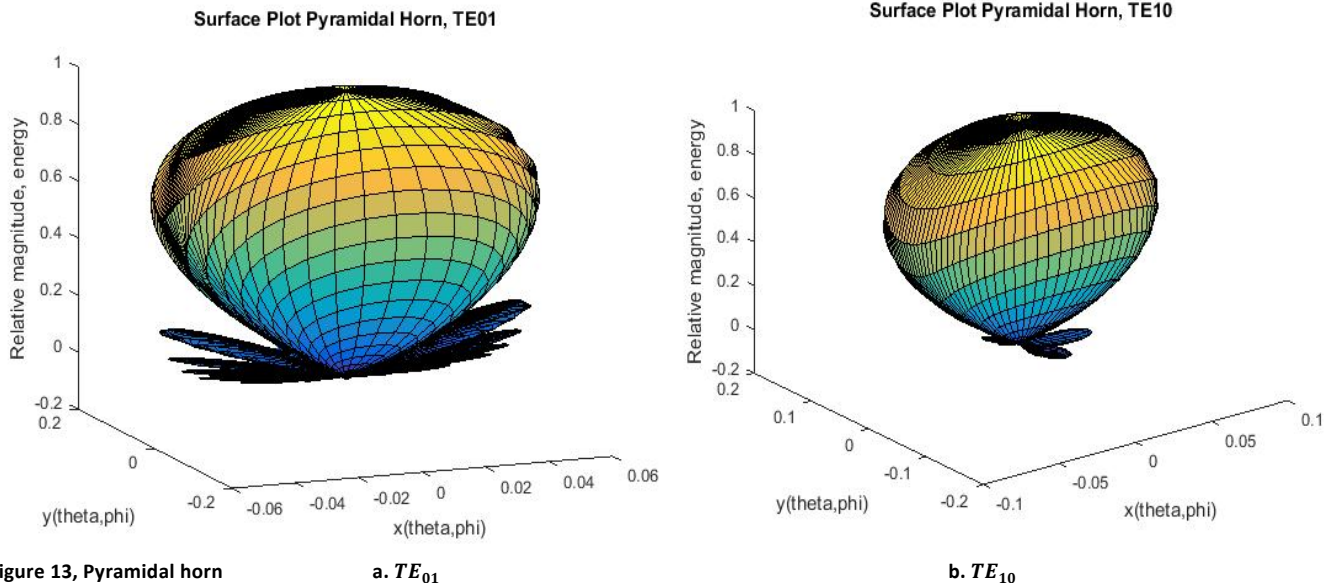
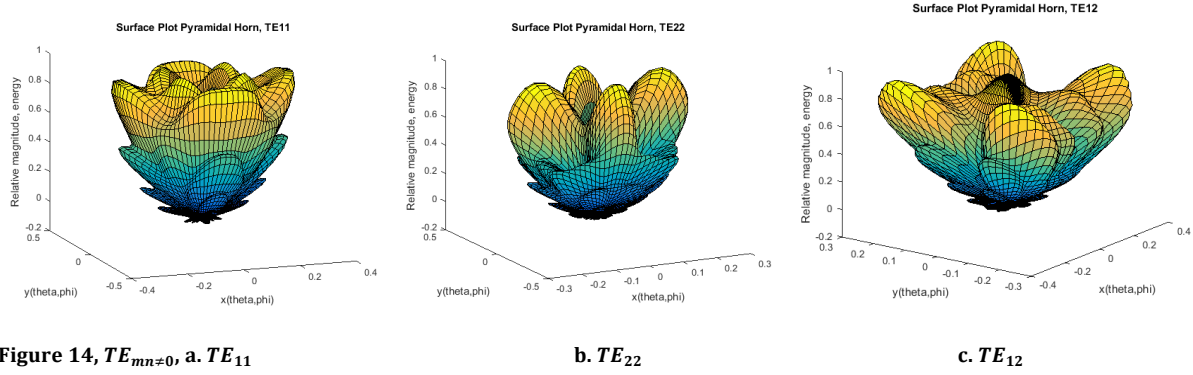


Figure 12, surface plot fundamental mode

The most common design of horn antennas are square aperture antennas for manufacturing reasons. For square aperture antennas, degenerate modes occur. Degenerate modes are modes with the same cut off frequency. Radiation patterns of degenerate modes are equivalent by a rotation of $\frac{\pi}{4}$. This property is shown for a pyramidal horn of the following dimensions: $a_1 = b_1 = 5.5\lambda$ and $\rho_1 = \rho_2 = 60\lambda$.



TE_{m0} and TE_{0n} modes have only an electric field in the axial directions, while TE_{mn} modes with $m, n \neq 0$ have contributions in both directions as given in figure 5. The radiation pattern of three cases are shown to understand the pattern.



Computational method

The software used to develop the wanted code is MATLAB. The code contains 150 rows. It is meant to plot any asked mode with any dimensions of a pyramidal horn antenna. The equation used to make the plots contains a double integral, equation [14]. The integral is solved analytically. The solution of the integral contains the Fresnel integrals. These integrals are left for MATLAB to solve. The script takes about a minute to solve the task. This calculation time is faster compared with design software which takes a day to give the same simulations. The advantage of the code is its simplicity, which make it easy to analyze and edit it. A disadvantage is the repeated calculations if some indices are changed.

This calculation time could be even shorter if approximation equations are used for the Fresnel integrals instead of the analytic solution by MATLAB. Because of the limited time spend on this thesis, the new code has not been finished.

This approximation equation⁹ could be used to make the code work faster.

$$C(x) = \int_0^x \cos \frac{\pi}{2} t^2 dt = \frac{1}{2} + f(x) \sin \frac{\pi}{2} t^2 - g(x) \cos \frac{\pi}{2} t^2 \quad [24]$$

$$\text{Where } f(x) = \frac{1+0.926}{2+1.792x+3.104x^2} + \epsilon(x), \quad g(x) = \frac{1}{2+14.142x+3.492x^2+6.67x^3} + \epsilon(x) \quad , \epsilon(x) \approx 0$$

The next step would be a code that summate many radiation patterns in one graph. This would be the applied form of equation [17]. For the same reason above, this code is not ready.

The script is given in the appendix.

⁹ Article, Computation of Fresnel Integrals

Discussions and Conclusions

In this thesis, the description of the fundamental mode is used as given in Antenna Theory by C. Balanis. This formulation is extended to contain higher order modes as explained in the article by Murphy and Padman. In this article, an expression is given wrongly. Because of this, the equation obtained for the higher order modes is wrong, too. The exponent on the right-hand side of equation (8) of the same article must be a plus instead of a minus. The final form of the equation is expected to be reducible to the fundamental mode for the values $m = 1, n = 0$. By replacing this mistake, the final equation derived is correct and is reducible to the equations given in Antenna Theory for the fundamental mode.

Furthermore, the way the radiation patterns are plotted is explained. The plots are the absolute values of the total electric field distribution which has components in the x and y directions. If square apertures are used with $m = n$, then both TE and TM radiation patterns become undistinguishable. This is illustrated by using equation [23] with $m = n$.

Lastly, a property of the fundamental mode is to radiate the biggest percentage of its energy in the main direction. This means that higher modes distribute their energy mainly in other directions and contribute a small amount to the main direction. If all modes are propagating in the horn, a large horn compared to wavelength, then the same amount of energy is radiated everywhere in space surrounding the antenna. This point is not presented graphically, because the script is only able to plot the patterns together independently instead of adding them together. Possible additional research in the future could make the script more advanced.

References

- [1] Balanis, C.A., 2nd edition, Antenna Theory analysis and design, Arizona State University, John Wiley & Sons, INC, New York.
- [2] J.A. Murphy, R. Padman, 1990, Radiation Patterns of Few-moded Horns and Condensing Lightpipes, Infrared Phys. Vol. 31, No. 3, pp. 291-299, St. Patrick's College, Maynooth.
- [3] Mairead Bevan, May 2013, Electromagnetic Analysis of Horn Antennas in the Terahertz region, Department of Experimental Physics, NUI Maynooth Ireland, Master Thesis.
http://eprints.maynoothuniversity.ie/4486/1/MaireadBevan_MScThesis.pdf
- [4] Hecht, H., 2014, Optics, 4th edition, Pearson New International Edition, United States of America.
- [5] Milenz, K.D., 1997, Computation of Fresnel Integrals, Journal of Research of the National Institute of Standards and Technology, Vol. 102, Number 3.
- [6] Whites, E.E., 2013, Microwave Engineering, Online Lecture 10
<http://whites.sdsmt.edu/classes/ee481/>
<http://whites.sdsmt.edu/classes/ee481/notes/481Lecture10.pdf>
- [7] Online Applet, www.amanogawa.com, 2015, Module 8.5, Rectangular Waveguide,
<http://www.amanogawa.com/archive/RectWaveGuide/RectWaveGuide.html>

Appendix

1. Derivation of equations [20] and [21]

The electromagnetic modes are described by goniometric function with arguments. The arguments are integer multiples of $\left(\frac{\pi}{\text{length of aperture}} \text{ variable}\right)$.

$$E_1 = \cos \frac{m\pi x}{a} \sin \frac{n\pi y}{b} \quad E_2 = \sin \frac{m\pi x}{a} \cos \frac{n\pi y}{b}$$

The derivation is done for E_1 following the article written by Murhy.

$$TE: E^{TE} = A \left[\frac{n}{b} E_1 \hat{i} + \frac{m}{a} E_2 \hat{j} \right] \quad TM: E^{TM} = A \left[\frac{m}{a} E_1 \hat{i} - \frac{n}{b} E_2 \hat{j} \right]$$

Which results in: $E_{total} = \iint 'mode' \left\{ \exp -ik \left(\frac{x^2}{\rho_2} + \frac{y^2}{\rho_1} \right) \right\} \{ \exp -ik(\cos \theta \sin \phi + \sin \theta \sin \phi) \} dx dy$

The boundaries of the integrals are $-\frac{a_1}{2}, \frac{a_1}{2}$ and $-\frac{b_1}{2}, \frac{b_1}{2}$. a and b are the dimension of the aperture of the antenna. Sometimes these are labeled in a different way. In Antenna Theory, the dimensions of the aperture of the pyramidal horn are a_1 and b_1 .

$$E_{total,1} = \iint E_1 \left\{ \exp -ik \left(\frac{x^2}{\rho_2} + \frac{y^2}{\rho_1} \right) \right\} \{ \exp -ik(\cos \theta \sin \phi + \sin \theta \sin \phi) \} dx dy$$

Divide this expression into two parts, I_1 and I_2 .

$$I_1 = \int \cos \frac{m\pi x}{a} \exp -ik \left(\frac{x^2}{\rho_2} \right) \exp -ik(\cos \theta \sin \phi) dx$$

$$I_2 = \int \sin \frac{n\pi y}{b} \exp -ik \left(\frac{y^2}{\rho_1} \right) \exp -ik(\sin \theta \sin \phi) dy$$

So $E_{total,1} = I_1 I_2$, with both I_1 and I_2 divided into two parts.

$$I_1 = I_1' + I_1'' \quad I_2 = I_2' + I_2''$$

This comes from the development of the goniometric equations in terms of exponents.

$$\sin x = \frac{(\exp ix - \exp -ix)}{2i} \quad \cos x = \frac{(\exp x + \exp -ix)}{2}$$

These $I_{1,2}'$ and $I_{1,2}''$ are giving respectively in the following rows.

$$\begin{aligned}
I_1' &= \exp \left\{ -i \left[\frac{kx^2}{2\rho_2} - xk_x'' \right] \right\} \exp \left(\frac{im\pi}{2} \right) & I_1'' &= \exp \left\{ -i \left[\frac{kx^2}{2\rho_2} - xk_x' \right] \right\} \exp \left(\frac{-im\pi}{2} \right) \\
I_2' &= \exp \left\{ -i \left[\frac{ky^2}{2\rho_1} - yk_y'' \right] \right\} \exp \left(\frac{in\pi}{2} \right) & I_2'' &= \exp \left\{ -i \left[\frac{ky^2}{2\rho_1} - yk_y' \right] \right\} \exp \left(\frac{-in\pi}{2} \right) \\
I_1 &= I_1' + I_1'' = \frac{1}{2} \left\{ \exp \left\{ -i \left[\frac{kx^2}{2\rho_2} - xk_x'' \right] \right\} \exp \left(\frac{im\pi}{2} \right) + \exp \left\{ -i \left[\frac{kx^2}{2\rho_2} - xk_x' \right] \right\} \exp \left(\frac{-im\pi}{2} \right) \right\} \\
I_2 &= I_2' + I_2'' = \frac{1}{2i} \left\{ \exp \left\{ -i \left[\frac{ky^2}{2\rho_1} - yk_y'' \right] \right\} \exp \left(\frac{in\pi}{2} \right) - \exp \left\{ -i \left[\frac{ky^2}{2\rho_1} - yk_y' \right] \right\} \exp \left(\frac{-in\pi}{2} \right) \right\}
\end{aligned}$$

With

$$\begin{aligned}
k_x'' &= k \sin \theta \cos \phi - \frac{m\pi}{a} & k_x' &= k \sin \theta \cos \phi + \frac{m\pi}{a} \\
k_y'' &= \sin \theta \sin \phi - \frac{n\pi}{b} & k_y' &= k \sin \theta \sin \phi + \frac{n\pi}{b}
\end{aligned}$$

Developing the integral gives the following expression:

$$\begin{aligned}
I_1' &= \sqrt{\frac{\pi\rho_2}{k}} \exp i \left(\frac{k_x''^2 \rho_2}{2k} \right) F_1 \\
F_1 &= [\mathcal{C}(t_2'') - \mathcal{C}(t_1'')] - i[S(t_2'') - S(t_1'')] \\
t_2'' &= \sqrt{\frac{1}{\pi k \rho_2}} \left(\frac{ka}{2} - k_x'' \rho_2 \right) & t_1'' &= \sqrt{\frac{1}{\pi k \rho_2}} \left(-\frac{ka}{2} - k_x'' \rho_2 \right)
\end{aligned}$$

So far the first part of the total form of the equation is completely done. The following parts, however, follow the same line of derivation.

$$\begin{aligned}
I_1'' &= \sqrt{\frac{\pi\rho_2}{k}} \exp i \left(\frac{k_x'^2 \rho_2}{2k} \right) F_2 \\
I_2' &= \sqrt{\frac{\pi\rho_1}{k}} \exp i \left(\frac{k_y''^2 \rho_1}{2k} \right) F_3 & I_2'' &= \sqrt{\frac{\pi\rho_1}{k}} \exp i \left(\frac{k_y'^2 \rho_1}{2k} \right) F_4
\end{aligned}$$

So the previous equations are now summarized in the next equation:

$$E_1 = \frac{\pi}{k} \sqrt{\rho_2 \rho_1} \left\{ \exp i \left(\frac{k_x''^2 \rho_2}{2k} \right) F_1 + \exp i \left(\frac{k_x'^2 \rho_2}{2k} \right) F_2 \right\} \left\{ \exp i \left(\frac{k_y''^2 \rho_1}{2k} \right) F_3 - \exp i \left(\frac{k_y'^2 \rho_1}{2k} \right) F_4 \right\}$$

E_2 follows the same procedure as above. The final form of E_2 is:

$$E_2 = \frac{\pi}{k} \sqrt{\rho_2 \rho_1} \left\{ \exp i \left(\frac{k_x''^2 \rho_2}{2k} \right) F_1 - \exp i \left(\frac{k_x'^2 \rho_2}{2k} \right) F_2 \right\} \left\{ \exp i \left(\frac{k_y''^2 \rho_1}{2k} \right) F_3 + \exp i \left(\frac{k_y'^2 \rho_1}{2k} \right) F_4 \right\}$$

Derivation of TE_{10} : The fundamental case is included in the above formula, for $m = 1$ and $n = 0$. Filling in these two value makes $E^{TM} = 0$ and $E^{TE} = A \left[\frac{E_2}{a} \hat{j} \right]$, so the remaining term is

$$E_{total} = Constant \left[\iint \sin \frac{m\pi x}{a} \exp -ik \left(\frac{x^2}{2L_x} + \frac{y^2}{2L_y} \right) \exp -ikr \, dx \, dy \right]^2$$

Evaluating the integrals give the following expression

$$\begin{aligned} E_{10}^{TE} = & \frac{\pi}{2k} \sqrt{L_x L_y} \left\{ F_1 e^{-i(k \sin \theta \cos \phi - \frac{x}{a}) \frac{L_x}{2k}} - F_2 e^{-i(k \sin \theta \cos \phi + \frac{x}{a}) \frac{L_x}{2k}} \right\} F_3 e^{-i(k \sin \theta \sin \phi) \frac{L_y}{2k}} \\ & \frac{\pi \sqrt{L_x L_y}}{k} \left\{ \exp \left(i(\sin \theta \sin \phi)^2 \frac{L_x}{2k} \right) F \right\} \left\{ \exp \left(i \left(\sin \theta \cos \phi - \frac{\pi}{a} \right)^2 \frac{L_x}{2k} \right) (F_1 - F_2) \right. \\ & \left. + \exp \left(i \left(\sin \theta \cos \phi + \frac{\pi}{a} \right)^2 \frac{L_x}{2k} \right) (-F_3 + F_4) \right\} \end{aligned}$$

Which is the fundamental mode as given in literature.

2. Sectoral Horn

Sectoral horns radiates only in one direction, only E or H plane is detectable.

$$|E_{total,sectoral}| = \frac{a\sqrt{\pi k \rho_1} E_1}{8r} \left| (1 + \cos \phi) F(t_1, t_2) \frac{\cos \left(\frac{k_x a}{2} \right)}{\left(\frac{k_x a}{2} \right)^2 - \left(\frac{\pi}{a} \right)^2} \right|$$

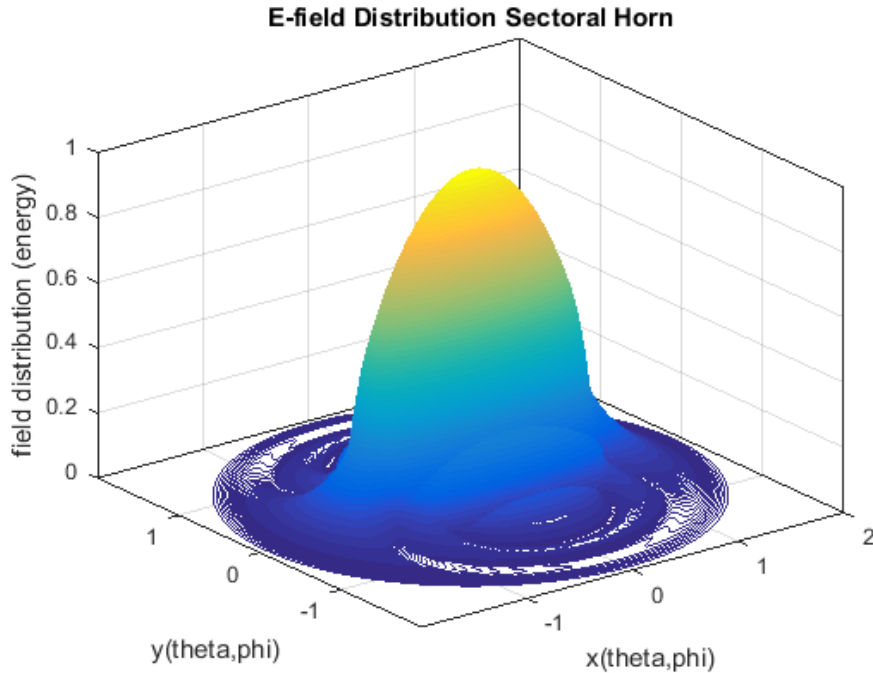


Figure 15, Sectoral horn, $a = 0.5\lambda$ and $b_1 = 2.75\lambda$

3. Script

a. To plot the modes

```
% Author H. Arbely
% Netherlands Institute of Space Research, SRON
% Physics Department @ University of Groningen, The Netherlands
%
% This scripts make plots of higher modes separately
% Input values are: dimension of aperture of antenna, wavelength, axial
% lengths rho1 and rho2

% Pyramidal horn antenna
% July 2015

clear all

% Parameters in units of lambda
a1= input('Give the value of a1 in terms of lambda: ');
%dimensions of aperture
b1= input('Give the value of b1 in terms of lambda: ');
rho1= input('Give the value of rho1 in terms of lambda: ');      %for x-
axis
rho2= input('Give the value of rho2 in terms of lambda: ');      %for y-
axis
m= input('Give the value of m: ');
n= input('Give the value of n: ');
lambda=1;
klambda=2*pi/lambda;

theta=linspace(0,pi,100);          % space is defined
phi=linspace (0,2*pi,100);
[Theta,Phi]=meshgrid(theta,phi);

c = @(x) cos((pi/2)*x.^2);    %FRESNEL FUNCTION,
s = @(x) sin((pi/2)*x.^2);    %FRESNEL FUNCTION,

kx1=(klambda*sin(Theta).*cos(Phi)+m*pi/a1);
kx2=(klambda*sin(Theta).*cos(Phi)-m*pi/a1);
ky1=(klambda*sin(Theta).*sin(Phi)+n*pi/b1);
ky2=(klambda*sin(Theta).*sin(Phi)-n*pi/b1);

k=1;                                %loop 1, Integral
bounadaries
j=1;

for theta_int=theta
    for phi_int=phi

        t1= sqrt(1/(klambda*rho1*pi))*(-klambda*a1/2-
(klambda*sin(theta_int)*cos(phi_int)+m*pi/a1)*rho1);      %kx2
```

```

        t2= sqrt(1/(klambda*rho1*pi))*(+klambda*a1/2-
(klamba*sin(theta_int)*cos(phi_int)+m*pi/a1)*rho1);

        t3= sqrt(1/(klambda*rho2*pi))*(-klambda*b1/2-
(klamba*sin(theta_int)*sin(phi_int)+n*pi/b1)*rho2);           %ky2
        t4= sqrt(1/(klambda*rho2*pi))*(+klambda*b1/2-
(klamba*sin(theta_int)*sin(phi_int)+n*pi/b1)*rho2);

        t5= sqrt(1/(klambda*rho1*pi))*(-klambda*a1/2-
(klamba*sin(theta_int)*cos(phi_int)-m*pi/a1)*rho1);           %kx1
        t6= sqrt(1/(klambda*rho1*pi))*(+klambda*a1/2-
(klamba*sin(theta_int)*cos(phi_int)-m*pi/a1)*rho1);

        t7= sqrt(1/(klambda*rho2*pi))*(-klambda*b1/2-
(klamba*sin(theta_int)*sin(phi_int)-n*pi/b1)*rho2);           %ky1
        t8= sqrt(1/(klambda*rho2*pi))*(+klambda*b1/2-
(klamba*sin(theta_int)*sin(phi_int)-n*pi/b1)*rho2);

        C    =integral(c,0,t2)-integral(c,0,t1);
        S    =integral(s,0,t2)-integral(s,0,t1);

        CC   =integral(c,0,t4)-integral(c,0,t3);
        SS   =integral(s,0,t4)-integral(s,0,t3);

        CCC  =integral(c,0,t6)-integral(c,0,t5);
        SSS  =integral(s,0,t6)-integral(s,0,t5);

        CCCC =integral(c,0,t8)-integral(c,0,t7);
        SSSS =integral(s,0,t8)-integral(s,0,t7);

        F3(k,j) =C    -1i *    S;           %F5 & F7 as defined in
derivation in essay
        F4(k,j) =CC   -1i *   SS;           %F4 & F8
        F1(k,j) =CCC  -1i *  SSS    ;       %F1 & F3
        F2(k,j) =CCCC -1i *SSSS;         %F2 & F6

        k=k+1;
        if(k>length(phi))

            k=1;
        end
    end
    j=j+1;
end

k=1;           %loop 2, to plot values > pi/2
j=1;

for theta_int=theta
    for phi_int=phi

        if theta_int > pi/2
            X(k,j)=(2-sin(theta_int)).*cos(phi_int);
            Y(k,j)=(2-sin(theta_int)).*sin(phi_int);

```



```

        else
            X(k,j)=sin(theta_int).*cos(phi_int);
            Y(k,j)=sin(theta_int).*sin(phi_int);

        end
        k=k+1;

        if(k>length(phi))
            k=1;

        end
    end
    j=j+1;
end

I1=
exp(1i*kx1.^2*rho1/(2*klambda)).*exp(1i*ky1.^2*(rho2/(2*klambda))).*F3.*F4*exp(1i*pi*(m+n)/2)/1i; % contributions of final equation
I2=
exp(1i*kx1.^2*rho1/(2*klambda)).*exp(1i*ky2.^2*(rho2/(2*klambda))).*F3.*F2*exp(1i*pi*(m-n)/2)/1i;
I3=
exp(1i*kx2.^2*rho1/(2*klambda)).*exp(1i*ky1.^2*(rho2/(2*klambda))).*F1.*F4*exp(1i*pi*(-m+n)/2)/1i;
I4=
exp(1i*kx2.^2*rho2/(2*klambda)).*exp(1i*ky2.^2*(rho2/(2*klambda))).*F1.*F2*exp(-1i*pi*(m+n)/2)/1i;

E_1 = ((pi*sqrt(rho1*rho2)/(4*1i*klambda))*((I1)+(I2)-(I3)-(I4)).*(1+cos(Theta)));
E_2 = ((pi*sqrt(rho1*rho2)/(4*1i*klambda))*((I1)-(I2)+(I3)-(I4)).*(1+cos(Theta)));

E_total1=abs(sqrt((abs(E_1)*m/a1).^2+(abs(E_2)*n/b1).^2));
E_total2=abs(sqrt((abs(E_1)*n/b1).^2+(abs(E_2)*m/a1).^2));

A1=max(max(E_total1)) ; % to plot the relativized graphs
D1=E_total1/A1;
A2=max(max(E_total2)) ;
D2=E_total2/A2;

Z=10*log10(D1);
K=Theta*180/pi;

hold on

figure(1) % Contour Plot
contour3(X,Y,D1,1000) % D1 for TE, D2 for TM
title(['E-field distribution Pyramidal Horn, TE' int2str(m),int2str(n)])
xlabel('x(theta,phi)')
ylabel('y(theta,phi)')
zlabel('Relative magnitude, energy')

```

```

figure (2)                                % Surface Plot
surface(Dl.*sin(Theta).*cos(Phi),Dl.*sin(Theta).*sin(Phi),Dl.*cos(Theta))
title(['Surface Plot Pyramidal Horn, TE' int2str(m),int2str(n)])
xlabel('x(theta,phi)')
ylabel('y(theta,phi)')
zlabel('Relative magnitude, energy')

%%% END

```

b. To plot the logarithmic scales

```

% Author H. Arbely
% Netherlands Institute of Space Research, SRON
% Physics Department @ University of Groningen, The Netherlands
%
% This scripts make plots of higher modes separately
% Input values are: dimension of aperture of antenna, wavelength, axial
% lengths rho1 and rho2

% Pyramidal horn antenna
% July 2015

clear all

% Parameters in units of lambda

lambda=1;
a=0.5;
b=0.25;
a1=12;
b1=6;

rho1=6;
rho2=6;
m=1;
n=0;

klambda=2*pi/lambda;

theta=linspace(-pi,pi,100);
phi=0;
phi2=pi/2;
[Theta,Phi]=meshgrid(theta,phi);

%t1= -((1/2)+sin(Theta)*sin(Phi));           %GRENZEN VAN DE INTEGRAAL
%t2= +((1/2)-sin(Theta)*sin(Phi));           %GRENZEN VAN DE INTEGRAAL

c = @(x) cos((pi/2)*x.^2);    %FRESNEL FUNCTIE, MATLAB HOORT DIT TE HERKENNEN
%q = integral(fun,0,t1);
s = @(x) sin((pi/2)*x.^2);    %FRESNEL FUNCTIE, MATLAB HOORT DIT TE HERKENNEN

kx1=(klambda*sin(Theta).*cos(Phi)-m*pi/a1);
kx11=(klambda*sin(Theta).*cos(Phi2)-m*pi/a1);

```

```

kx2=(klambda*sin(Theta).*cos(Phi)+m*pi/a1);
kx22=(klambda*sin(Theta).*cos(Phi2)+m*pi/a1);
ky1=(klambda*sin(Theta).*sin(Phi)-n*pi/b1);
ky11=(klambda*sin(Theta).*sin(Phi2)-n*pi/b1);
ky2=(klambda*sin(Theta).*sin(Phi)+n*pi/b1);
ky22=(klambda*sin(Theta).*sin(Phi2)+n*pi/b1);

k=1;
j=1;

for theta_int=theta
    for phi_int=phi

        t1= sqrt(1/(klambda*rho1*pi))*(-klambda*a1/2-
(klamba*sin(theta_int)*cos(phi_int)+m*pi/a1)*rho1); %kx2
        t2= sqrt(1/(klambda*rho1*pi))*(+klambda*a1/2-
(klamba*sin(theta_int)*cos(phi_int)+m*pi/a1)*rho1);

        t3= sqrt(1/(klambda*rho2*pi))*(-klambda*b1/2-
(klamba*sin(theta_int)*sin(phi_int)+n*pi/b1)*rho2); %ky2
        t4= sqrt(1/(klambda*rho2*pi))*(+klambda*b1/2-
(klamba*sin(theta_int)*sin(phi_int)+n*pi/b1)*rho2);

        t5= sqrt(1/(klambda*rho1*pi))*(-klambda*a1/2-
(klamba*sin(theta_int)*cos(phi_int)-m*pi/a1)*rho1); %kx1
        t6= sqrt(1/(klambda*rho1*pi))*(+klambda*a1/2-
(klamba*sin(theta_int)*cos(phi_int)-m*pi/a1)*rho1);

        t7= sqrt(1/(klambda*rho2*pi))*(-klambda*b1/2-
(klamba*sin(theta_int)*sin(phi_int)-n*pi/b1)*rho2); %ky1
        t8= sqrt(1/(klambda*rho2*pi))*(+klambda*b1/2-
(klamba*sin(theta_int)*sin(phi_int)-n*pi/b1)*rho2);

        C=integral(c,0,t2)-integral(c,0,t1);
        S=integral(s,0,t2)-integral(s,0,t1);

        CC=integral(c,0,t4)-integral(c,0,t3);
        SS=integral(s,0,t4)-integral(s,0,t3);

        CCC=integral(c,0,t6)-integral(c,0,t5);
        SSS=integral(s,0,t6)-integral(s,0,t5);

        CCCC=integral(c,0,t8)-integral(c,0,t7);
        SSSS=integral(s,0,t8)-integral(s,0,t7);

        F3(k,j)=C      -1i *    S;
%F5 & F7
        F4(k,j)=CC     -1i *    SS;
%F4 & F8
        F1(k,j)=CCC    -1i *    SSS;
%F1 & F3
        F2(k,j)=CCCC  -1i *    SSSS;
%F2 & F6

```

```

        k=k+1;
        if(k>length(phi))

            k=1;
        end
    end
    j=j+1;
end

k=1;
j=1;

for theta_int=theta
    for phi_int=phi

        if theta_int > pi/2
            X(k,j)=(2-sin(theta_int)).*cos(phi_int);

            Y(k,j)=(2-sin(theta_int)).*sin(phi_int);
        else
            X(k,j)=sin(theta_int).*cos(phi_int);

            Y(k,j)=sin(theta_int).*sin(phi_int);

        end
        k=k+1;

        if(k>length(phi))
            k=1;

        end
    end
    j=j+1;
end

I1=
exp(1i*kx1.^2*rho1/(2*klambda)).*exp(1i*ky1.^2*(rho2/(2*klambda))).*F1.*F2*exp(1i*pi*(m+n)/2)/1i;
I2=
exp(1i*kx1.^2*rho1/(2*klambda)).*exp(1i*ky2.^2*(rho2/(2*klambda))).*F1.*F4*exp(1i*pi*(m-n)/2)/1i;
I3=
exp(1i*kx2.^2*rho1/(2*klambda)).*exp(1i*ky1.^2*(rho2/(2*klambda))).*F3.*F2*exp(1i*pi*(-m+n)/2)/1i;
I4=
exp(1i*kx2.^2*rho2/(2*klambda)).*exp(1i*ky2.^2*(rho2/(2*klambda))).*F3.*F4*exp(-1i*pi*(m+n)/2)/1i;

E_1 = abs((pi*sqrt(rho1*rho2)/(4*1i*klambda))*((I1)+(I2)-(I3)-(I4)).*(1+cos(Theta)));
E_2 = abs((pi*sqrt(rho1*rho2)/(4*1i*klambda))*((I1)-(I2)+(I3)-(I4)).*(1+cos(Theta)));

E_totall=abs(sqrt(((E_1)*m/a1).^2+((E_2)*n/b1).^2));

```

```

E_total2=abs(sqrt((E_1*n/b1).^2+(E_2*m/a1).^2));
A=max(max(E_total1))
% to plot the log graph
D=E_total1/A;
Z=10*log10(D);
K=Theta*180/pi;

hold on

figure(1)
plot(K,Z)
title(['Intensity , TE' int2str(m),int2str(n)])
xlabel('Theta (angles)')
ylabel('Intensity (dB)')

figure(2)
plot(K,Z)
title(['Intensity , TE' int2str(m),int2str(n)])
xlabel('Theta (angles)')
ylabel('Intensity (dB)')

legend('E-plane','H-plane')

% END

```